

A Temperature Window of Reduced Flow Resistance in Polyethylene: In Situ WAXS

H. M. M. van Bilsen,^{*,†} H. Fischer,[†] J. W. H. Kolnaar,[‡] and A. Keller[§]

Centre for Polymers and Composites (CPC), Faculty of Chemical Engineering and Chemistry, Eindhoven University of Technology, P.O. Box 513, 5600 MB Eindhoven, The Netherlands, DSM Research, P.O. Box 18, 6160 MD Geleen, The Netherlands, and H. H. Wills Physics Laboratory, University of Bristol, Bristol, United Kingdom

Received April 4, 1995; Revised Manuscript Received July 31, 1995[®]

ABSTRACT: During extended capillary flow, a melt flow singularity for polyethylene occurs in a narrow temperature interval close to 150 °C. This was revealed by a minimum in pressure for constant material throughput. In situ X-ray experiments show only one distinct sharp reflection for polyethylene under these particular conditions. This single reflection was clearly different from the reflections from the orthorhombic phase, and more important, it appears while all orthorhombic reflections vanish. Possibly, the single reflection observed corresponds to a mobile phase which may act as a kind of lubricant for the bulk polyethylene. This mobile phase could reduce the melt flow resistance and therefore induce the extrusion window of reduced flow resistance.

Introduction

During capillary flow of linear polyethylene, a melt flow singularity occurs in a narrow temperature interval close to 150 °C.¹ This is revealed by a minimum in pressure for constant material throughput and a maximum in material throughput when a constant pressure is maintained.² In the former case the temperature window sets in at a critical piston velocity while in the latter at a critical pressure. Within this narrow temperature interval, a minimum in extrusion pressure is accompanied by smooth extrudability and comparatively little die swell, resulting in smooth extrudates without gross distortions. The potential advantages of this processing window are apparent either by melt properties³⁻⁵ or by that of the resulting solidified product, e.g., toughness, fracture, and wear improvement.⁶ On both sides of the temperature window, extrusion is very irregular. Polymer processing instabilities have been described extensively by continuum rheology. Nevertheless, our experiments propose a different approach to elucidate the temperature window of reduced flow resistance in polyethylene.

Figure 1 demonstrates the invariance of temperature at the pressure minimum with extrusion rate and the requirement of a critical shear rate.^{1,4} This temperature is well above its maximum theoretical melting temperature of 145 °C.⁷ Moreover, being confined to a narrow temperature interval of ± 1 °C, the origin of the "extrusion window" points to a thermodynamic factor induced by chain extension. By constraining the molecules in an elongational state, the configurational entropy of the molten state lowers S_L and hence G_L ($G_L = H_L - TS_L$) and successive phase transition temperatures raise.⁸ As a result, chains can be stabilized in highly oriented polymers against melting by favoring the low-entropy fibrillar state against the high-entropy melt.⁹

During capillary flow, chain extension is expected to take place as a result of elongational flow at the converging die entrance. Van der Vegt and Smit¹⁰ found unusually high orientation within the capillary and

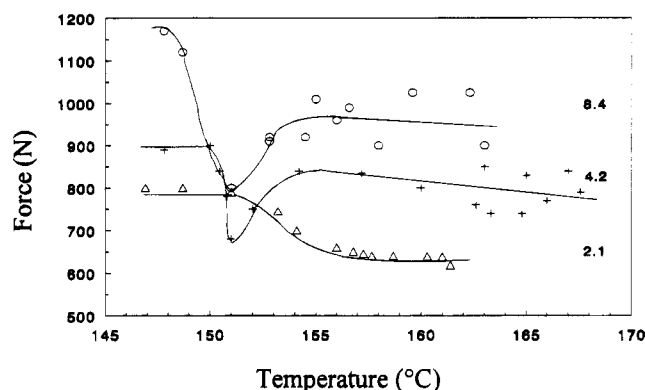


Figure 1. Piston force vs temperature traces showing the onset of the pressure minimum with increasing shear rate (s^{-1}).

suggested that the elevated crystallization temperature of polyethylene resulted from orientation-induced crystallization. Hence polyethylene crystallizes at elevated temperatures and flow diminishes eventually giving rise to complete blockage of flow due to the formation of orthorhombic crystals. This is contrary to the presently observed phenomena, where the flow rate increases in the processing interval. Therefore, it has been hypothesized that the observed effect requires a phase that is slippery and hence possesses mobile polymer chains.

At ambient and stationary conditions, polyethylene possesses orthorhombic crystals. However, applying high pressure^{9, 11} or application of external constraints during melting of a highly oriented polyethylene fiber¹² can result in a stable two-dimensional hexagonal crystal structure. This phase has an anomalously high longitudinal mobility of the polymer chains.¹¹

The slippery phase described might agree with a hexagonal phase arising through flow-induced chain extension. Previous in situ wide-angle X-ray scattering (WAXS) experiments revealed a weak crystalline reflection in the form of a small shoulder. However, the extrusion window occurred at lower temperatures, and due to limits of intensity and registration sensitivity, it could not be conclusive regarding the nature of the reflections.¹³

In this study, similar in situ WAXS experiments on polyethylene have been performed to reveal the differ-

[†] Eindhoven University of Technology.

[‡] DSM Research.

[§] University of Bristol.

[®] Abstract published in *Advance ACS Abstracts*, October 15, 1995.

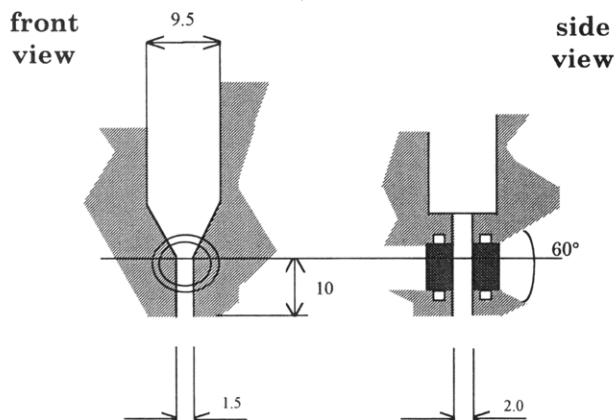


Figure 2. Experimental setup of capillary rheometer with slit geometry.

ences in crystal structures between solidified material at room temperature and during extended capillary flow within the extrusion window. Experiments were performed using a capillary rheometer with a slit geometry and X-ray-transparent beryllium windows.¹³ This rheometer was built by DSM Research in collaboration with H. G. Zachman, S. Seifert, and C. Zsunke from the University of Hamburg.

Experimental Section

(a) Materials. The linear polyethylene investigated was HD6720pr200 ($M_w = 280 \text{ kg} \cdot \text{mol}^{-1}$, $M_w/M_n = 7.5$) provided by DSM (Geleen, The Netherlands) as a fine powder.

(b) Sample Preparation. Material. The powder was molten for 30 min at 180 °C and continuously condensed in the cylindrical reservoir of the capillary rheometer. Subsequently the molten polymer was cooled till a constant preset temperature was reached.

Capillary Extrusion. In situ X-ray diffraction extrusion experiments were performed on a specially built capillary rheometer with a slit geometry mounted on a piston extruder. The experimental set up consisted of a 9.5 mm diameter cylindrical reservoir of 160 mm length and a slit-shaped die (Figure 2, taken from ref 17). The dimensions of the capillary were $L \times W \times D = 10.0 \times 1.5 \times 2.0 \text{ mm}^3$, and the entry of the capillary converged from 9.5×2.0 to $1.5 \times 2.0 \text{ mm}^2$ with an entry angle of 90°. The die was equipped with a set of 10 mm diameter X-ray-transparent beryllium windows, each of 2.0 mm thickness. Moreover, at the exit of the beam, a conical aperture of 60° was employed enabling double Bragg reflection angles up to $2\theta = 30^\circ$ to be detected.

Both piston speed and capillary temperature could be controlled independently. During extrusion experiments, the piston force was continuously monitored at a constant piston speed. Both isothermal and "dynamic" experiments were conducted. In the latter case, the capillary temperature was increased stepwise.

(c) Characterization Techniques. WAXS measurements were conducted at HASYLAB, Deutsches Elektronen Synchrotron (DESY), Hamburg, Germany. At ambient temperature, electrons were accelerated using a synchrotron and subsequently injected into storage rings.¹⁴ After monochromization and collimation, a beam with a wavelength of $\lambda = 0.154 \text{ nm}$ and size of approximately $2 \times 0.5 \text{ mm}^2$ was produced. WAXS diffraction patterns ($13^\circ \leq 2\theta \leq 32^\circ$) were collected with a linear position-sensitive detector equipped with 512 channels. Due to space limitations, the available 1D detector was positioned vertically beneath the incident beam. The channel number was calibrated against the double Bragg reflection angles of the 110 ($2\theta = 21, 74^\circ$) and 200 ($2\theta = 24, 18^\circ$) reflections of solidified polyethylene at room temperature.¹⁵ By mounting a long russell, a distance of around 50 cm between WAXS detector and sample was obtained, providing the best resolution possible. Each experiment was performed

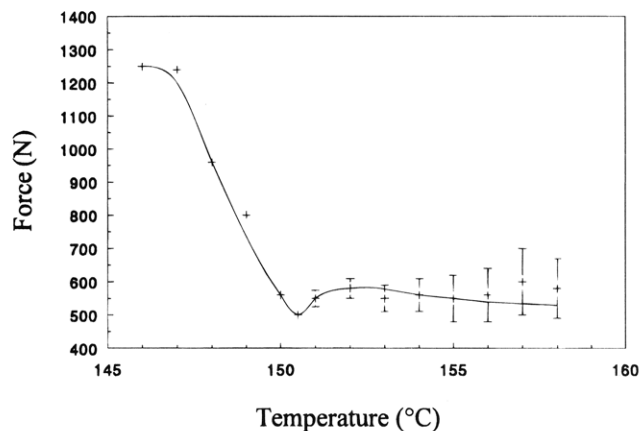


Figure 3. Piston force vs temperature plot of extruding polyethylene through a slit geometry die.

on a sample with a thickness of 2 mm and a data acquisition time of 15–30 s. By adjusting the position of the capillary rheometer with respect to the beam, the best intensity was obtained.

All results describing the relevant phases involved in the anomalous flow were computed from the obtained scattering data using the OTOKO¹⁶ program package. After correction for detector response and subtraction of the background, the obtained reflections were assigned using Lorentz curve profiles in the PEAKFIT program (Jandel Scientific Software). Only the amorphous halo was fitted by a Gaussian curve. The statistical r -values for the best fit were close to 1.

Orientation measurements were carried out at the edge and the bulk of the solidified extrudates within the window. Samples were prepared by cutting thin sections, of approximately $50\text{--}100 \mu\text{m}$, from the edge at room temperature with a Reichert Ultracut E microtome, whereas the remaining extrudate was referred to as bulk material. WAXS patterns were obtained using an Elliot GX 21 rotating anode generator with a copper target equipped with a flat graphite crystal monochromator and a collimator comprising two pairs of crossed slits. The detection device was a Siemens X-1000 area detector coupled with a PC (GADDS software) for collecting, analyzing, and storing WAXS images. Subsequently, the azimuthal intensity distribution of the (200)₀ was computed in order to obtain the Herman's orientation factor of the crystalline phase using

$$f_H = \frac{3 \langle \cos^2 \phi \rangle - 1}{2} \quad (1)$$

where

$$\langle \cos^2 \phi \rangle = \frac{\int_0^{\pi/2} I(\phi) \sin \phi \cos^2 \phi \, d\phi}{\int_0^{\pi/2} I(\phi) \sin \phi \, d\phi} \quad (2)$$

Results and Discussion

(a) The Principle Effect: Extrusion Window with Slit Geometry. Capillary die extrusion revealed the pronounced influence of temperature on extrusion pressure. Figure 3 presents a typical piston force vs temperature behavior well above the critical shear rate¹³ (piston speed $35 \text{ mm} \cdot \text{min}^{-1}$) for this setup. Commencing extrusion at 146 °C and continuously heating the viscous melt with a heating rate of $2 \text{ }^\circ\text{C} \cdot \text{min}^{-1}$ demonstrates a narrow temperature interval in which the extrusion pressure became anomalously low with a minimum pressure located around 150 °C. At higher temperatures, pressure oscillations became more pronounced resulting an unstable pressure level.

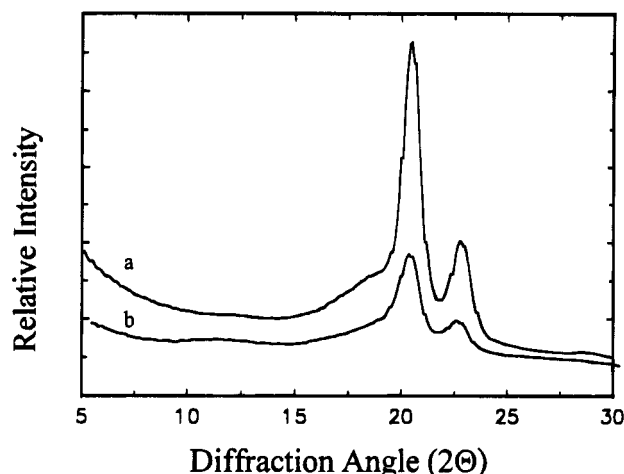


Figure 4. WAXS intensity vs double Bragg reflection at $T = 23 \pm 1$ °C for (a) polyethylene and (b) polyethylene with beryllium windows.

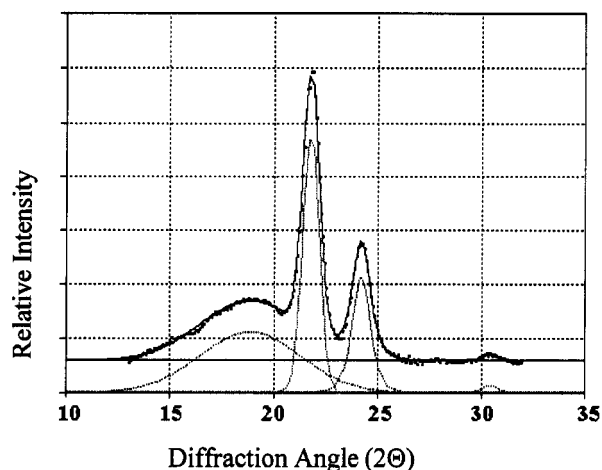


Figure 5. Relative WAXS intensity vs double Bragg reflection angle at $T = 23 \pm 1$ °C for polyethylene without flow.

In addition to the piston force curve, the singularity of the window is characterized by the appearance of the extrudate in the temperature range from 146 to 160 °C. Both die swell and surface smoothness show a dramatic change with temperature. Initially, the material shows a high die swell ratio ($d_{\text{strand}}/d_{\text{die}}$) with a maximum of approximately 2.5. The smoothness relating to the window temperature is noticeable by the absence of die swell. Progressive heating results in pronounced surface distortions and nonuniformities, with the strand emerging in spurts.¹⁷

To determine the X-ray transparency of beryllium, Figure 4 shows the corrected WAXS data of solid polyethylene at room temperature. Clearly, the beryllium windows only reduced the intensity of the diffraction pattern. No significant discrepancies were observed both for the orthorhombic peak positions and for the resolution.

Consequently, the capillary rheometer with slit geometry and beryllium windows can be used for X-ray experiments to reveal the subsequent crystal structures of polyethylene during extrusion.

(b) Morphological Changes within the Extrusion Window. Figure 5 shows the corrected data of the WAXS curve of a solid polyethylene sample at room temperature. The sample was crystallized from the melt within the capillary die and clearly gives rise to a broad reflection at $2\theta \approx 18.5^\circ$ corresponding to the

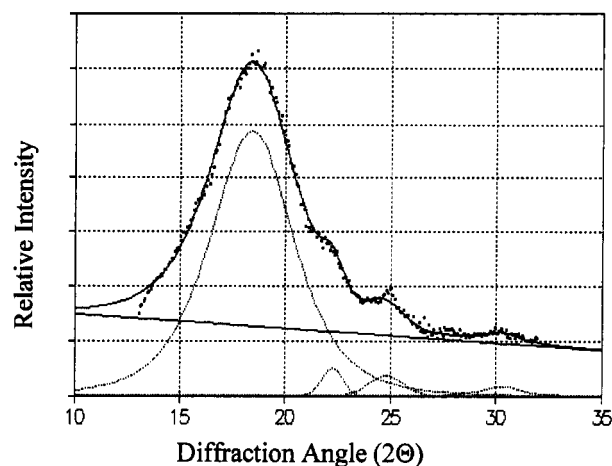


Figure 6. Relative WAXS intensity vs double Bragg reflection angle at $T = 149 \pm 1$ °C for polyethylene; flow = $35 \text{ mm} \cdot \text{min}^{-1}$.

Table 1. Peak Position Obtained from Figures 5–7

source	sample	T (°C)	Bragg reflecting (deg)				
			110 _o	200 _o	210 _o	???	amo
Figure 5	solidified	23	21.7	24.2	30.3		18.7
Figure 6	extruded	149	21.7	24.7	30.0		18.4
Figure 7	extruded	150				20.9	18.4

amorphous bulk material. Two intense orthorhombic reflections appear originating from the (200) and (110) planes in addition to the weaker (210) reflection. For calibration, the orthorhombic (110) reflection was taken to be at $2\theta = 21.73^\circ$ and the (200) reflection at $2\theta = 24.18^\circ$. Consequently the (210) reflection is assigned to $2\theta \approx 30^\circ$, as consistent with literature.^{12,18}

Upon heating, the Bragg reflections of the orthorhombic phase only slightly shift (Table 1). Apparently, heating of polyethylene from room temperature to 149 °C (commencing extrusion at 146 °C) hardly influences the orthorhombic periodicity. However, it is evident that the intensities of these reflections decrease significantly on increasing temperature. This can be clearly depicted by comparing Figure 5 and Figure 6.

This observation is in full agreement with previous work of Pennings¹² in a bundle of strained polyethylene macrofibers, Rastogi⁹ in highly oriented UHMWPE gel-spun fibers, and Ryan et al.¹⁸ on a molded PE sheet. They observed that, on heating polyethylene, all orthorhombic reflections diminish in intensity. More important, around 150 °C all three orthorhombic reflections vanish instantaneously.

Figure 7 depicts the WAXS intensity for polyethylene at 150 °C, during extrusion within the extrusion window. Strikingly, besides the amorphous scattering, only one distinct reflection is observed, $2\theta = 0.8^\circ$ below the (110) orthorhombic one. Simultaneously, the position of the amorphous halo is not shifted (Table 1). The change in position, assuming this single reflection would be the (110) of the orthorhombic phase, cannot be explained in terms of extrusion forces. Such a shift would require much higher pressure differences.

The appearance of a single reflection upon heating polyethylene has been observed during experiments using, e.g., highly oriented samples.^{12,18,19} Besides the orthorhombic reflections at lower temperatures, all recorded diffraction patterns show one additional reflection around 150 °C. This single reflection has been attributed to a hexagonal packing of chains. Subsequently, raising temperature by a few degrees, all three

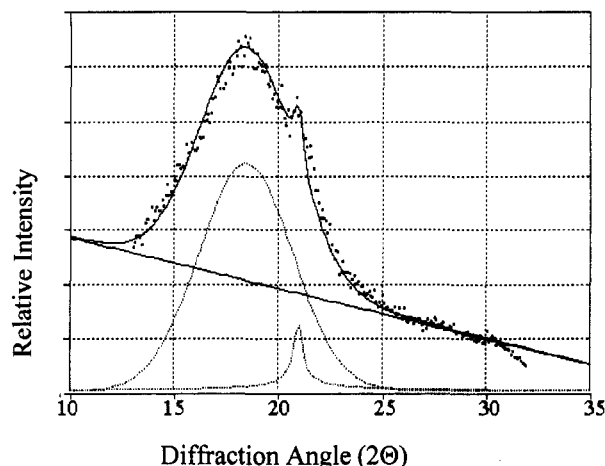


Figure 7. Relative WAXS intensity vs double Bragg reflection angle at $T = 150 \pm 1$ °C for polyethylene; flow = $35 \text{ mm} \cdot \text{min}^{-1}$.

orthorhombic reflections disappear simultaneously, whereas the additional hexagonal reflection strengthens.

Strikingly, our experiments reveal the same. At 150 °C, Figure 7 reveals only a single reflection. Therefore, it is impossible to attribute this reflection to an orthorhombic crystal. However, this single reflection is present in a short temperature range, only inside the extrusion window. Since capillary flow is not as strong a constraint as in the cases mentioned before,^{12,18,19} these weaker constraints will cause a smaller temperature region of stability for the newly formed phase.

The extrusion window appears at a specific, sharply defined temperature, which points to the presence of a phase transition. Furthermore, the newly formed phase should be connected with the formation of a mobile "slippery" conformation since orthorhombic crystals would block the capillary.¹⁰ To reveal this metastable slippery phase, its melting temperature has to be elevated to a greater extent than the stable one. In general, by chain extension, a temperature range can be created with a stable slippery phase. In the case of a hexagonal structure, the larger distance between polymer chains allows chain rotation around their *c*-axes. Moreover, the increased volume available for the chains in the hexagonal phase may give rise to relaxation of pressure as a result of slippage of polymer molecules with respect to each other. This randomization of the chains in the subsequent stage of constrained melting will be accompanied by several trans-gauche formations.²⁰ As a result, a more mobile phase is obtained in comparison to the orthorhombic^{20,21} one.

(c) Orientation within the Extrusion Window. Previous rheological studies suggest that the origin of the extrusion window resides in the capillary at or near the wall as a result of slippage.¹⁷ However, simple shear flow should not extend chains significantly. On the other hand, chain extension could occur as a result of shear flow when molecules are anchored at the walls as in the case of adsorption. This is described in recent theory from Brochard and de Gennes.²² For sparsely adsorbed chains there is a critical velocity at which these chains disentangle. The anchored chains extend to what they term a "marginal state" with an associated slip larger along the walls. Such a situation was observed experimentally with chains purposefully attached to the surface.²³ At the appropriate temperature, such extended chains then could possibly be transformed in a mobile phase. This would then coincide

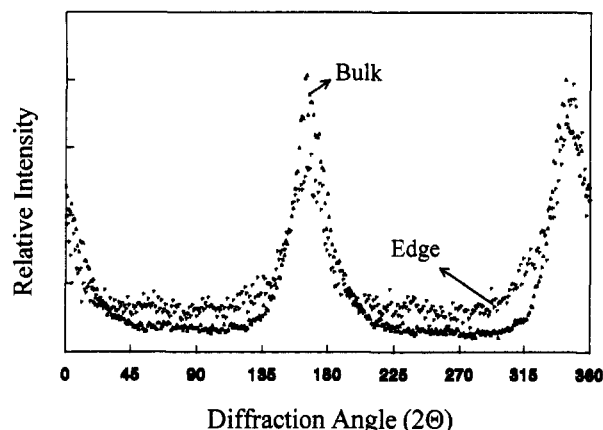


Figure 8. Azimuthal intensity distribution of the $(020)_0$ reflection for (a) bulk material and (b) edge material.

with our WAXS experiments. This slippery surface could act as a lubricant for the bulk polyethylene. Consequently, slippage of the material at or in close vicinity to the solid boundary could convert a Poiseuille-type flow behavior into partial plug flow.

Figure 8 demonstrates azimuthal intensity distribution curves for the $(200)_0$ reflection of both edge and bulk material after crystallization. Clearly, both samples are oriented with no significant difference in the Herman orientation factor (bulk 0.74; edge 0.70), which coincides with plug flow. However, the Herman orientation factor is obtained from the crystalline part alone whereas orientation in the amorphous part is not taken into account. Moreover, since orientation is not determined from in situ experiments, relaxation has to be kept in mind.

Conclusions

In situ WAXS experiments were performed on polyethylene during extrusion using a slit-shaped capillary. In a narrow temperature interval close to 150 °C, the described melt flow singularity was revealed by a minimum in pressure for constant material throughput. Simultaneously, clearly one distinct reflection has been observed different from the reflections expected for the orthorhombic phase. Most important, this reflection appeared while all orthorhombic reflections disappeared. This excludes the presence of the orthorhombic phase, since all three reflections should be present as stated earlier.

The results presented here may contribute to clarify the temperature window of reduced flow resistance in polyethylene during capillary flow. Possibly, the single reflection observed corresponds to a mobile phase, which may act as a kind of lubricant at the surface of the bulk polyethylene. This slippery phase could reduce the melt flow resistance and therefore induce the extrusion window of reduced flow resistance.

Acknowledgment. Besides support from DSM Research, Geleen, The Netherlands, for material supply and use of the capillary rheometer, the financial contribution of 3M Co. Saint Paul is gratefully acknowledged. The authors are also grateful to Prof. H. G. Zachman and his group for the facilities of HASYLAB, Deutsches Elektronen Synchrotron (DESY), Hamburg, Germany. Special thanks for the use of the area detector, Polymer Group, H. H. Wills Physics Laboratory, University of Bristol, United Kingdom.

References and Notes

- (1) Waddon, A. J.; Keller, A. *J. Polym. Sci.* **1992**, *30*, 923.
- (2) Kolnaar J. W. H.; Keller A. *Polymer* **1994**, *35*, 3863.
- (3) Waddon, A. J.; Keller, A. *J. Polym. Sci.* **1990**, *28*, 1063.
- (4) Narh, K. A.; Keller, A. *Polymer* **1991**, *32*, 2512.
- (5) Narh, K. A.; Keller, A. *J. Mater. Sci. Lett.* **1991**, *10*, 1301.
- (6) Bashir, Z.; Odell, J. A. *J. Mater. Sci.* **1993**, *28*, 1081.
- (7) Flory, P. J.; Vrij, A. *J. Am. Chem. Soc.* **1963**, *85*, 3548.
- (8) Keller, A.; Ungar G.; Percec V. *ACS Symp. Ser.* **1990**, No. 435, 308.
- (9) Rastogi, S.; Odell, J. A. *Polymer* **1993**, *34*, 1523.
- (10) van der Vegt, A. K.; Smit, P. P. A. *Adv. Polym. Sci. Techn., Soc. Chem. Ind.* **1967**, *26*, 313.
- (11) Bassett, D. C.; Block, S.; Piermarini, G. J. *J. Appl. Phys.* **1974**, *45*, 4146.
- (12) Pennings A. J.; Zwiijnenburg A. J. *Polym. Sci., Polym. Phys. Ed.* **1979**, *17*, 1011.
- (13) Kolnaar, J. W. H.; Keller, A., submitted for publication in *Polym.*
- (14) Elsner, G.; Riekel Ch.; Zachmann, H. G. *Adv. Polym. Sci.* **1984**, *67*, 3.
- (15) Walter, N. M.; Reding, J. *J. Polym. Sci.* **1956**, *21*, 561.
- (16) Program developed by DESY staff, for collecting, storing, and processing of X-ray data.
- (17) Kolnaar, J. W. H.; Keller, A. *Polymer* **1995**, *36*, 821.
- (18) Ryan, A. J.; et al. *Polymer* **1994**, *21*, 4537.
- (19) Hikmet R.; Keller, A., unpublished results.
- (20) Stroble, G.; et al. *J. Chem. Phys.* **1974**, *61*, 5257 and 5265.
- (21) Bonsor, D. H.; Bloor D. *J. Mater. Sci.* **1977**, *12*, 1552.
- (22) Brochard, F.; de Gennes, P. G. *Langmuir* **1992**, *8*, 3033.
- (23) Migler, K. B. Massey, G., Hervet, H., Leger, L. *J. Phys. Condens. Matter* **1994**, *6*, A30.1.

MA950450P